Reactivity of a Vanadium(III) Center over an Oxo Surface Modeled by Calix[4]arene

Barbara Castellano, Euro Solari, Carlo Floriani,* and Rosario Scopelliti

Institut de Chimie Minérale et Analytique, BCH, Université de Lausanne, CH-1015 Lausanne, Switzerland

Nazzareno Re

Facoltà di Farmacia, Università degli Studi "G. D'Annunzio", I-66100 Chieti, Italy

Received January 6, 1999

Metalation of the monomethoxycalix[4]arene [*p*-Bu^t-calix[4]-(OMe)(OH)$_3$], **1**, using [VMes$_3$·THF] led to the coordinatively unsaturated V^{III}-d^2 fragment [*p*-Bu^t-calix[4]-(OMe)(O)$_3$V] collapsing to the dimer [{μ-*p*-Bu^t-calix-[4]-(OMe)(O)$_3$}V]$_2$, **2**, where each calix[4]arene shares a bridging oxygen donor atom. The dimeric complexity remains intact in the reaction with Bu^{t}NC and PhCN, which bond to the metal inside the cavity of the calix[4]-arene leading to [{μ-*p*-Bu^t-calix[4]-(OMe)(O)$_3$}(V−L)]$_2$ [L = Bu^{t}NC, **3**; L = PhCN, **4**]. In contrast, the reaction of **2** with pyridine and 4,4′-dipyridyl cleaves the dimeric form into a monomeric complex [{μ-*p*-Bu^t-calix[4]-(OMe)(O)$_3$}V(Py)], **5**, or to a different dimer containing a bridging 4,4′-dipyridyl, [{*p*-Bu^t-calix[4]-(OMe)(O)$_3$}$_2$V$_2$-(μ-4,4′-dipyridyl)], **6**. Complex **2** undergoes one electron oxidation by I$_2$ to the corresponding vanadium(IV) dimer [{μ-*p*-Bu^t-calix[4]-(O)$_4$}$_2$V$_2$], **7**, and by *p*-benzoquinone to [{*p*-Bu^t-calix[4]-(OMe)(O)$_3$}V]$_2$(μ-C$_6$H$_4$O$_2$), **8**. A two-electron oxidation of the V^{III}-d^2 to vanadium(V) derivatives has been achieved using styrene epoxide and diphenyldiazomethane. In the former case the oxovanadium(V) derivative was obtained [*p*-Bu^t-calix[4]-(OMe)-(O)$_3$V═O], **9**, and in the latter case a metallahydrazone complex [*p*-Bu^t-calix[4]-(OMe)(O)$_3$V≡N−N═CPh$_2$], **10**. The dimeric d^2 and d^1 derivatives display significant antiferromagnetic couplings between the two metal centers, namely as follows: **2**, $J = -74.6$ cm^{-1}; **3**, $J = -17$ cm^{-1}; **4**, $J = -33.4$ cm^{-1}; **7**, $J = -131.7$ cm^{-1}. The extended Hückel calculations gave an appropriate picture of the two-electron reduction of the diphenyldiazomethane substrate. The proposed structures have been supported by X-ray analyses on **3**, **7**, **9**, and **10**.

Introduction

The generation of electron-rich metals over a quasiplanar binding surface made up exclusively of oxygen donor atoms would allow us to mimic rather closely the topology and the activity of heterogeneous metal oxide surfaces.[1,2] Our recent molecular approach in this field used a preorganized O$_4$ set of donor atoms derived from the deprotonated form of calix[4]-arene[3] and its alkylated derivatives.[4] A parallel and quite significant molecular approach for mimicking an oxo surface has been made by Feher, who used silsesquioxanes as ancillary ligands to better understand the nature of the active silica-supported metal and, in particular, vanadium species.[5] The two

* To whom correspondence should be addressed.

(1) (a) Thomas, J. M.; Thomas, W. J. *Principles and Practice of Heterogeneous Catalysis*; VCH: Weinheim, Germany, 1997. (b) *Mechanisms of Reactions of Organometallic Compounds with Surfaces*; Cole-Hamilton, D. J., Williams, J. O., Eds.; Plenum: New York, 1989. (c) Kung, H. H. *Transition Metal Oxides: Surface Chemistry and Catalysis*, Elsevier: Amsterdam, The Netherlands, 1989. (d) Hoffmann, R. *Solid and Surfaces, A Chemist's View of Bonding in Extended Strucures*; VCH: Weinheim, Germany, 1988. (e) *Catalyst Design, Progress and Perspectives*; Hegedus, L., Ed.; Wiley: New York, 1987. (f) Bond, G. C. *Heterogeneous Catalysis, Principles and Applications*, 2nd ed.; Oxford University Press: New York, 1987.

(2) For related molecular approaches to oxo surfaces binding organometallic functionalities see: (a) Chisholm, M. H. *Chemtracts−Inorg. Chem.* **1992**, *4*, 273. (b) Kläui, W. *Angew. Chem., Int. Ed. Engl.* **1990**, *29*, 627. (c) Nagata, T.; Pohl, M.; Weiner, H.; Finke, R. G. *Inorg. Chem.* **1997**, *36*, 1366. (d) Pohl, M.; Lyon, D. K.; N. Mizuno, N.; Nomiya, K.; Finke, R. G. *Inorg. Chem.* **1995**, *34*, 1413.

(3) (a) Gutsche, C. D. *Calixarenes*; The Royal Society of Chemistry: Cambridge, U.K., 1989. (b) *Calixarenes, A Versatile Class of Macrocyclic Compounds*; Vicens, J., Böhmer, V., Eds.; Kluwer: Dordrecht, The Netherlands, 1991. (c) Bohmer, V. *Angew. Chem., Int. Ed. Engl.* **1995**, *34*, 713.

(4) (a) Giannini, L.; Solari, E.; Zanotti-Gerosa, A.; Floriani, C.; Chiesi-Villa, A.; Rizzoli, C. *Angew. Chem., Int. Ed. Engl.* **1996**, *35*, 85. (b) Giannini, L.; Solari, E.; Zanotti-Gerosa, A.; Floriani, C.; Chiesi-Villa, A.; Rizzoli, C. *Angew. Chem., Int. Ed. Engl.* **1996**, *35*, 2825. (c) *Angew. Chem., Int. Ed. Engl.* **1997**, *36*, 753. (d) Giannini, L.; Caselli, A.; Solari, E.; Floriani, C.; Chiesi-Villa, A.; Rizzoli, C.; Re, N.; Sgamellotti, A. *J. Am. Chem. Soc.* **1997**, *119*, 9198. (e) *Ibid.* **1997**, *119*, 9709. (f) Giusti, M.; Solari, E.; Giannini, L.; Floriani, C.; Chiesi-Villa, A.; Rizzoli, C. *Organometallics* **1997**, *16*, 5610. (g) Zanotti-Gerosa, A.; Solari, E.; Giannini, L.; Floriani, C.; Chiesi-Villa, A.; Rizzoli, C. *J. Am. Chem. Soc.* **1998**, *120*, 437. (h) Giannini, L.; Solari, E.; Floriani, C.; Chiesi-Villa, A.; Rizzoli, C. *J. Am. Chem. Soc.* **1998**, *120*, 823. (i) Zanotti-Gerosa, A.; Solari, E.; Giannini, L.; Floriani, C.; Re, N.; Chiesi-Villa, A.; Rizzoli, C. *Inorg. Chim. Acta* **1998**, *270*, 298. (j) Caselli, A.; Giannini, L.; Solari, E.; Floriani, C.; Re, N.; Chiesi-Villa, A.; Rizzoli, C. *Organometallics* **1997**, *16*, 5457. (k) Castellano, B.; Zanotti-Gerosa, A.; Solari, E.; Floriani, C.; Chiesi-Villa, A.; Rizzoli, C. *Organometallics* **1996**, *15*, 4894. (l) Gardiner, M. G.; Lawrence, S. M.; Raston, C. L.; Skelton, B. W.; White, A. H. *Chem. Commun.* **1996**, 2491. (m) Gardiner, M. G.; Koutsantonis, G. A.; Lawrence, S. M.; Nichols, P. J.; Raston, C. L. *Chem. Commun.* **1996**, 2035. (n) Gibson, V. C.; Redshaw, C.; Clegg, W.; Elsegood, M. R. J. *J. Chem. Soc., Chem. Commun.* **1995**, 2371. (o) Acho, J. A.; Doerrer, L. H.; Lippard, S. J. *Inorg. Chem.* **1995**, *34*, 2542.

(5) (a) Feher, F. J.; Newman, D. A.; Walzer, J. F. *J. Am. Chem. Soc.* **1989**, *111*, 1741. (b) Feher, F. J.; Walzer, J. F. *Inorg. Chem.* **1991**, *30*, 1689. (c) Feher, F. J.; Walzer, J. F.; Blanski, R. L. *J. Am. Chem. Soc.* **1991**, *113*, 3618. (d) Feher, F. J.; Blanski, R. L. *J. Am. Chem. Soc.* **1992**, *114*, 5886. (e) Feher, F. J.; Blanski, R. L. *Organometallics* **1993**, *12*, 958. (f) Feher, F. J.; Budzichowski, T. A. *Polyhedron* **1995**, *14*, 3239 and references therein.

10.1021/ic990017m CCC: $18.00
Published on Web 06/24/1999

Chart 1

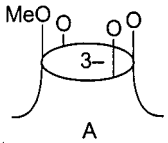

A
[*p*-Bu^t-calix[4]-(OMe)(O)$_3$]$^{3-}$

general synthetic procedures for the generation of electron-rich metals bonded to the calix[4]arene skeleton are (i) the metalation followed by the reduction of high valent metals and (ii) the direct metalation using organometallic precursors, such as homoleptic alkyl or aryl compounds. The latter methodology, avoiding the presence of halide anions derived from metathesis reaction, is also more appropriate for the generation of coordinatively unsaturated metals. The purpose of the work presented in this paper is to generate a V^{III}-d^2 on top of an O_4 set of oxygen donor atoms derived from a calix[4]arene skeleton. In this regard we found recently that d^2 and d^3 metallacalix[4]arene fragments are particularly suitable for assisting hydrocarbon rearrangements[4h] and dinitrogen reduction[4g] and for managing the chemistry of M−C, M=C, and M≡C functionalities.[4a−k] We have recently reported the chemistry of the vanadium−carbon bond functionalities over an oxo surface defined by the calix[4]arene skeleton, in particular the dimethoxycalix[4]arene dianion.[6] We report here the generation of a d^2-vanadium(III) coordinatively unsaturated species bonded to the monomethoxycalix[4]arene trianion (**A**) (Chart 1) and its oxidations to vanadium(IV) and vanadium(V). The chemical studies have been completed by a detailed magnetic analysis of the vanadium(III) and vanadium(IV) dimers and by an extended Hückel analysis.

Experimental Section

General Procedure. All reactions were carried out under an atmosphere of purified nitrogen. Solvents were dried and distilled before use by standard methods. Infrared spectra were recorded with a Perkin-Elmer FT 1600 spectrophotometer, and NMR spectra on AC-200E and DPX-400 Bruker instruments. Magnetic susceptibility measurements were made on an MPMS5 SQUID susceptometer (Quantum Design Inc.), operating at a magnetic field strength of 1 kOe. Corrections were applied for diamagnetism calculated from Pascal constants.[7] Effective magnetic moments were calculated as $\mu_{eff} = 2.828(\chi_V T)^{1/2}$, where χ_V is the magnetic susceptibility per vanadium. Fitting of the magnetic data to the theoretical expression was performed by minimizing the agreement factor, defined as

$$\sum \frac{[\chi_i^{obsd} T_i - \chi_i^{calcd} T_i]^2}{(\chi_i^{obsd} T_i)^2}$$

by a Levenberg−Marquardt routine. The syntheses of **1**[4i] and [$VMes_3$·THF][8] were carried out as reported elsewhere.

Synthesis of 2. 1 (6.9 g, 10.4 mmol) was added to a blue THF (200 mL) solution of [$VMes_3$·THF][8] (5.25 g, 10.50 mmol) at −20 °C. The solution was stirred for 2 h at room temperature and gave a green microcrystalline precipitate which was collected (6.4 g, 72%). Anal. Calcd for **2**·4THF, $C_{106}H_{142}O_{12}V_2$: C, 74.43; H, 8.38. Found: C, 74.27; H, 8.51.

Synthesis of 3. Bu^{t}NC (0.146 g, 1.75 mmol) was added to a green THF (200 mL) suspension of **2**·4THF (1.5 g, 0.875 mmol). The suspension was stirred for 12 h at room temperature. A light-brown microcrystalline solid was obtained, which was filtered out and collected (1.22 g, 78%). Anal. Calcd for **3**·4THF, $C_{116}H_{160}N_2O_{12}V_2$: C, 74.24; H, 8.61; N, 1.49. Found: C, 74.35; H, 8.54; N, 1.29. IR (Nujol, ν_{max}/cm^{-1}): 2197. Crystals suitable for X-ray analysis were grown from a toluene solution and contain toluene of crystallization.

Synthesis of 4. PhCN (0.18 g, 1.75 mmol) was added to a green THF (200 mL) suspension of **2**·4THF (1.5 g, 0.875 mmol). After a few hours a microcrystalline gray solid was obtained, which was filtered out and collected (1.21 g, 71%). Anal. Calcd for **4**·4THF, $C_{120}H_{152}N_2O_{12}V_2$: C, 75.19; H, 8.01; N, 1.46. Found: C, 75.42; H, 7.98; N, 1.5. IR (Nujol, ν_{max}/cm^{-1}): 1596 (m), 2274 (m-s).

Synthesis of 5. Pyridine (20 mL) was added to a green THF (120 mL) suspension of **2**·4THF (1.1 g, 0.64 mmol). After 1 h, the green suspension turned orange and a yellow-orange solid was collected (0.5 g, 81%). Anal. Calcd for **5**·2THF·0.5Py, $C_{60.5}H_{77.5}N_{1.5}O_6V$: C, 74.72; H, 7.97; N, 2.16. Found: C, 74.61; H, 7.87; N, 2.04. $\mu_{eff} = 3.35\ \mu_B$ at 298 K.

Synthesis of 6. 4,4′-Dipyridyl (0.29 g, 1.84 mmol) was added to a THF (200 mL) suspension of **2**·4THF (1.58 g, 0.92 mmol). The suspension immediately turned red. After 12 h, a red microcrystalline solid was collected (1.10 g, 64%). Anal. Calcd for **6**·4THF, $C_{116}H_{150}N_2O_{12}V_2$: C, 74.63; H, 8.12; N, 1.50. Found: C, 74.38; H, 7.86; N, 1.49. $\mu_{eff} = 3.15\ \mu_B$ at 298 K per vanadium.

Synthesis of 7. A THF solution (20 mL) of I_2 (0.19 g, 0.75 mmol) was added dropwise to a green THF suspension (200 mL) of **2**·4THF (1.28 g, 0.75 mmol) at room temperature. After 12 h of stirring, the solvent was removed in vacuo, and the red residue was extracted with *n*-hexane (150 mL). Deep-red crystals of the complex were obtained from the *n*-hexane solution (0.80 g, 70%). Anal. Calcd for **7**·3C_6H_{14}, $C_{106}H_{146}O_8V_2$, C, 76.92; H, 8.95. Found: C, 77.18; H, 8.85. A sample of the crude of the reaction was analyzed by CG-MS: CH_3I was identified.

Synthesis of 8. *p*-Benzoquinone (0.082 g, 0.76 mmol) was added to a green THF (200 mL) suspension of **2**·4THF (1.3 g, 0.76 mmol). The suspension immediately became a dark solution. Volatiles were removed in vacuo. *n*-Hexane (50 mL) was added to the dark red residue that was then collected as a brick red powder (0.9 g, 76%). Anal. Calcd for **8**, $C_{96}H_{120}O_{12}V_2$: C, 75.06; H, 7.09. Found: C, 75.13; H, 7.25. $\mu_{eff} = 1.75\ \mu_B$ at 298 K per vanadium.

Synthesis of 9. Styrene oxide (0.162 g, 1.35 mmol) was added to a green THF suspension of **2**·4THF (1.54 g, 0.675 mmol). The green suspension was refluxed for 12 h, and a dark solution was obtained. Volatiles were removed in vacuo. The brown solid was washed with *n*-hexane (60 mL) and collected as a brown powder (0.8 g, 82%). Anal. Calcd for **9**, $C_{45}H_{55}O_5V$: C, 74.38; H, 7.57. Found: C, 74.61; H, 7.92. ^{1}H NMR (C_6D_6, 298 K, ppm): 7.18 (d, 2H, $J = 2.44$ Hz, CH_{arom}); 7.15 (d, 2H, $J = 2.44$ Hz, CH_{arom}); 6.86 (s, 2H, CH_{arom}); 6.85 (s, 2H, CH_{arom}); 4.73 (d, 2H, $J = 12.68$ Hz, CH_2-calix); 4.27 (d, 2H, $J = 12.68$ Hz, CH_2-calix); 3.87 (s, 3H, OCH_3); 3.16 (d, 2H, $J = 12.68$ Hz, CH_2-calix); 3.12 (d, 2H, $J = 12.68$ Hz, CH_2-calix); 1.37 (s, 18H, Bu^t); 0.98 (s, 9H, Bu^t); 0.72 (s, 9H, Bu^t). ν(V=O, Nujol): 1026 cm^{-1}. Crystals were grown in a saturated solution of THF/Et_2O and contain THF and Et_2O of crystallization.

Synthesis of 10. Ph_2CN_2 (0.40 g, 2.08 mmol) was added to a THF (120 mL) green suspension of **2**·4THF (1.78 g, 1.04 mmol). After a few hours a dark solution was obtained. Volatiles were removed in vacuo. The dark residue was washed with pentane (60 mL) and collected as a black microcrystalline solid (1.3 g, 69%). Anal. Calcd for **10**, $C_{58}H_{65}N_2O_4V$: C, 76.95; H, 7.25; N, 3.09. Found: C, 77.38; H, 7.74; N, 2.87. ^{1}H NMR (C_6D_6, 298 K, ppm): 8.07 (bs, 2H, arom); 7.62 (bs, 2H, arom); 7.23 (s, 4H, arom); 7.14 (m, 6H, arom); 6.94 (s, 2H, arom); 6.90 (s, 2H, arom); 4.79 (d, 2H, $J = 12.2$ Hz, CH_2-calix); 4.50 (d, 2H, $J = 12.2$ Hz, CH_2-calix); 4.25 (s, 3H, OCH_3); 3.27 (d, 2H, $J = 12.2$ Hz, CH_2-calix); 3.26 (d, 2H, $J = 12.2$ Hz, CH_2-calix); 1.41 (s, 18H, Bu^t-calix); 0.84 (s, 9H,; Bu^t-calix); 0.75 (s, 9H, Bu^t-calix). Crystals suitable for X-ray analysis were obtained from a diluted pentane solution and contain pentane of crystallization.

(6) Castellano, B.; Solari, E.; Floriani, C.; Re, N.; Chiesi-Villa, A.; Rizzoli, C. *Organometallics* **1998**, *17*, 2328.
(7) Boudreaux, E. A.; Mulay, L. N. *Theory and Applications of Molecular Paramagnetism*; John Wiley: New York, 1976; pp 491−495.
(8) (a) Vivanco, M.; Ruiz, X.; Floriani, C.; Chiesi-Villa, A.; Rizzoli, C. *Organometallics* **1993**, *12*, 1794. (b) Vivanco, M.; Ruiz, X.; Floriani, C.; Chiesi-Villa, A.; Rizzoli, C. *Organometallics* **1993**, *12*, 1802. (c) Ruiz, X.; Vivanco, M.; Floriani, C.; Chiesi-Villa, A.; Rizzoli, C. *Organometallics* **1993**, *12*, 1811.

Table 1. Crystal Data and Structure Refinement for **3**, **7**, **9**, and **10**

	3	**7**	**9**	**10**
formula	$C_{100}H_{128}N_2O_8V_2 \cdot 2C_7H_8$	$C_{88}H_{104}O_8V_2 \cdot 3C_6H_{14}$	$C_{45}H_{55}O_5V \cdot 2C_4H_8O \cdot {}^1/_6C_4H_{10}O$	$C_{58}H_{65}N_2O_4V \cdot {}^3/_2C_5H_{12}$
fw	1772.19	1650.11	883.39	1013.28
T, K	143	143	143	190
λ, Å	1.541 78	0.710 73	0.710 73	0.710 70
cryst system	triclinic	triclinic	rhombohedral	monoclinic
space group	$P\bar{1}$	$P\bar{1}$	$R\bar{3}$	$P2_1/n$
a, Å	14.061(3)	12.639(3)	22.606(2)	12.563(3)
b, Å	14.676(3)	13.486(3)	22.606(2)	25.946(5)
c, Å	12.869(3)	15.108(3)	22.606(2)	18.535(4)
α, deg	100.21(3)	77.75(3)	113.152(10)	90
β, deg	90.95(3)	72.24(3)	113.152(10)	94.86(3)
γ, deg	70.96(3)	84.56(3)	113.152(10)	90
V, Å^3	2468.1(9)	2395.3(8)	7439.2(14)	6020(2)
Z	1	1	6	4
D_{calc}, g/cm^3	1.192	1.144	1.183	1.118
μ, mm^{-1}	2.031	0.249	0.250	0.211
reflcns collcd	5662	5434	28842	14262
data/params	5306/522	5116/509	7098/572	5505/595
$R1$ [$I > 2\sigma(I)$]	0.0860	0.0808	0.1109	0.0791
w$R2$	0.3519	0.2398	0.2688	0.2359

X-ray Crystallography for Complexes 3, 7, 9, and 10. Crystals of **3**, **7**, **9**, and **10** were mounted in glass capillaries and sealed under nitrogen. Crystal data and structure refinement details are listed in Table 1. Diffraction data for complex **3** and **7** were collected at 143 K on Rigaku AFC6S and AFC7S four-circle diffractometers, respectively, and then processed with teXsan for Windows release 1.0.1 (Molecular Structure Corp., a Rigaku Company, 3200 Research Forest Drive, The Woodlands, TX 77381-4238, 1997). Data for complex **9** were collected on a KUMA CCD at 143 K and then reduced with the use of KUMARED release 1.4.8 (Kuma Diffraction Instruments GmbH, PSE-EPFL module 3.4, CH-1015, Lausanne, Switzerland, 1998). Data for complex **10** were collected on a mar345 area detector and then processed with marHKL release 1.9.1.[9] No absorption correction was applied to any data set. The structures were solved by direct methods with the program SHELXS 97.[10] The refinement was carried out by full-matrix-block least squares on F^2 with all non-H atoms (except the carbon atoms belonging to the toluene molecule for **3**, half-hexane molecule for **7**, and the solvent molecules which are present in **10**) and refined anisotropically using the program SHELXL-97-2 PC version.[11] Hydrogen atoms (CH_3 hydrogens and solvent hydrogens, when present) were placed in calculated positions using the "riding model", with a common isotropic displacement parameter ($U_{iso} = 0.08$ Å^2), while aromatic and CH_2 hydrogens were allowed to ride on the parent carbon atom with $U_{iso} = 1.2U_{eq}$(C). In the last stage of refinement the weighting scheme adopted [$1/(\sigma^2(F_o^2) + (aP)^2 + bP$, where $P = (F_o^2+2F_c^2)/3$] gave the following result for a and b, respectively: 0.1792, 0.0000, **3**; 0.0802, 20.0314, **7**; 0.1105, 25.8534, **9**; 0.1450, 0.0000, **10**. The most relevant difficulties in the refinement of all the structures dealt with the presence of some solvent molecules that appeared to be affected by some disorder. Therefore some restraints/constrains were applied. In complex **3**, the toluene ring was fitted to a regular hexagon and assumed to be isotropic; absorption correction was not applied because the best result was achieved using the raw data. In complex **7**, the half-hexane molecule that lies on an crystallographic inversion center was assumed to be isotropic. In complex **9**, hydrogens were not localized on the half-ether molecule lying on a 3-fold axis. In complex **10**, the solvent was assumed to be isotropic and hydrogens were not placed on it. The final difference maps showed some electron density peaks, mostly close to the disordered solvent. Molecular graphics were done by XP.[12] Material for publication has been prepared with XCIF included in the SHELXTL software package[13] while geometrical calculations have been performed with SHELXL-97-2 PC version.[11] Final atomic coordinates for all atoms, thermal parameters, and bond distances and angles are listed in Tables S1−S20.[14] Ordering information is given on any current masthead page.

Scheme 1

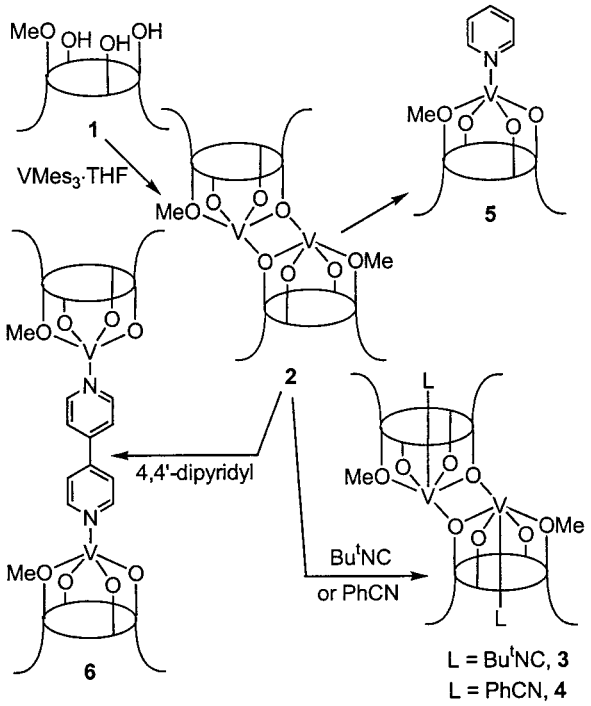

Results and Discussion

Chemical Studies. The bonding of a d^2-vanadium(III) to a calix[4]arene oxo surface was achieved reacting [$VMes_3$·thf][8] with **1**[4i] (Scheme 1). In the absence of any coordinating solvent, the reaction led to a dimer, where vanadium(III) achieves pentacoordination. The dimeric nature of **2** is supported by its magnetic behavior (see below), showing an antiferromagnetic coupling. The atom connectivity should not be much different from the solvated forms **3** and **4** obtained from **2** upon reaction

(9) Otwinowski, Z.; Minor, W. In *Methods in Enzymology, Volume 276: Macromolecular Crystallography*; Carter, C. W., Jr., Sweet, R. M., Eds.; Academic: New York, 1997; Part A, pp 307−326.
(10) Sheldrick, G. M. *Acta Crystallogr., Sect. A: Cryst. Phys,. Diffr., Theor. Gen. Crystallogr.* **1990**, *A46*, 467.
(11) Sheldrick, G. M. *Program for the Refinement of Crystal Structures*; University of Göttingen: Göttingen, Germany, 1998.
(12) Interactive Molecular Graphics, release 5.1, Bruker AXS, Inc., Madison, WI 53719, 1998.
(13) Bruker AXS, Inc., Madison, WI 53719, 1997.
(14) See paragraph at the end of paper regarding Supporting Information.

Scheme 2

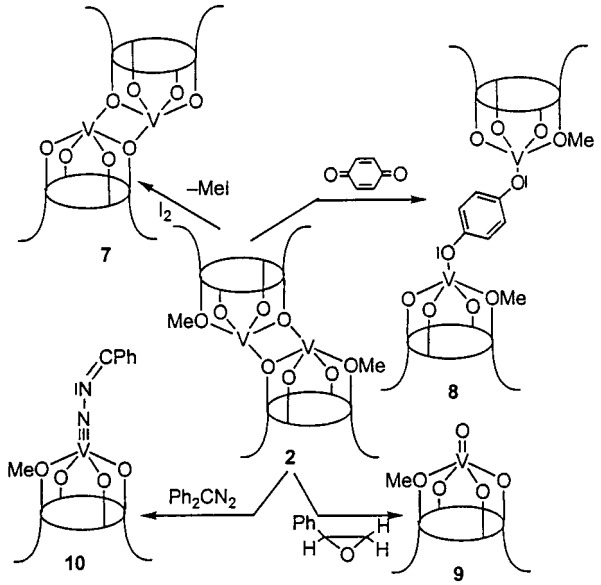

with Bu^{t}NC and PhCN, respectively. Such a reaction is a valid means to assemble the double cone structure **2** in supramolecular aggregates using guest molecules containing linear functionalities.[4i,6,15] The structure of **3** has been elucidated with an X-ray analysis (see below). The magnetic properties of **3** and **4** are rather similar (see below) to those of **2**, thus giving a strong support for its dimeric formulation. The preferential complexation to the metal inside the cavity shows the strong bridge-bonding mode of the calix[4]arene sharing a phenoxo oxygen. Cleavage, however, of the dimer occurs upon reaction with pyridine producing **5**. The magnetic properties of **5** are in agreement with its monomeric nature. The reaction with pyridine suggests to us how one can bridge two vanadium(III) centers via a ligand which can, eventually, ensure communication between the two paramagnetic centers. The reaction of **2** with 4,4′-dipyridyl led, in fact, to the formation of the dimer **6** which, however, did not show any magnetic interaction between the two paramagnetic centers.

The redox behavior of vanadium(III) is shown in Scheme 2. Monoelectronic oxidation has been achieved using I_2 and *p*-benzoquinone. In the former case, the oxidation of vanadium(III) to vanadium(IV) is followed by the nucleophilic displacement of the methyl from the methoxy group. Such a mechanism has been discussed in detail in some recent reports.[4i,k,6] The same compound **7** has been obtained via the oxidation of [{calix[4]-(OMe)$_2$(O)$_2$}V(*p*-MeC$_6$H$_4$)] with I_2.[6] The vanadium(IV) derivative **7** maintains the dimeric structure of **2**. Such a structure, which has been clarified by an X-ray analysis (see below), gives rise to a significant antiferromagnetic coupling between the d^1 configurations (see below). The reduction of *p*-benzoquinone to the hydroquinone dianion in the reaction with **2** is followed by the complexation to the vanadium(IV) centers with the cleavage of the dimeric structure and the formation of **9**.[16] Some preliminary X-ray and magnetic data are in agreement with the dimeric structure, which does not show any magnetic interaction between the two metal centers.

The vanadium(III)-d^2 centers react as a metal−carbenoid with the oxo transfer agents or diazoalkanes. In the former case, the oxidation of **2** to the diamagnetic oxovanadium(V), **9**, was achieved using the styrene oxide.[8b] Deoxygenation of epoxides by low-valent metals has a number of precedents.[17] The complex was both analytically and spectroscopically characterized, including X-ray analysis.[5,18,19] This type of chemical environment has been proposed for V═O in heterogeneous vanadium-based oxidation catalysts,[1] where the V═O unit is active in oxygen transfer processes.

The reaction of **2** with diphenyldiazomethane enters the game of the d^2 metals active in dinitrogen fixation and reduction.[20] As a matter of fact, diazoalkane complexes have been considered as models for the chemistry of N_2 fixation.[21] The four-electron reduction of N_2 to hydrazido tetraanion by a Nb(III)−calix[4]-arene fragment[4g] parallels the two electron reduction of diphenyldiazomethane in complex **10** or by some organometallic fragments.[22] The complex can be easily viewed as the condensation between the ketonic-like functionality V═O in **9** and the benzophenone hydrazone.

Structural Studies. The structures of the dimers **3** and **7** are displayed in Figures 1 and 2, with the numbering scheme reported in Chart 2. In both compounds the calix-4-arene moiety has a similar (Table 2) cone conformation, as expected for a hexacoordinate metal, complex **3**, having the *trans*-L$_2$MO$_4$ donor atom arrangement or for a five-coordinate metal as in complex **7**. The vanadium out of the O$_4$ plane varies from 0.003(6) in **3** to 0.310(3) Å in **7**. The V−O bond distances, which are diagnostic of the electron density at the metal, decrease remarkably (Table 3) from **3** to **7** according to the increase of the oxidation state of the metal [V^{III} → V^{IV}] and the high electronic density at the metal in the case of **3**, determined by the strong σ donor Bu^{t}NC. As a consequence the π-donation to the metal by the phenoxo group increases quite a bit moving from **3** to **7**. The other structural parameters are quite normal[6] (see the Supporting Information). The structures of the two monomeric vanadium(V) complexes are shown in Figures 3 and 4. In both complexes the metal is five-coordinate, thus maintaining the calix-4-arene fragment conelike conformation (Table 2) with a slight out of the O$_4$ plane of the metal [0.406(2), **9**;

(15) Zanotti-Gerosa, A.; Solari, E.; Giannini, L.; Floriani, C.; Chiesi-Villa, A.; Rizzoli, C. *Chem. Commun.* **1996**, 119.

(16) Crystal data for **8**: $C_{96}H_{114}O_{10}V_2$, $M = 1529.75$, triclinic, space group $P\bar{1}$, $a = 13.434(15)$ Å, $b = 20.52(2)$ Å, $c = 22.12(2)$ Å, $\alpha = 63.85(11)°$, $\beta = 82.60(9)°$, $\gamma = 83.98(11)°$, $V = 5421(10)$ Å^3, $Z = 2$, $D_{calcd} = 0.937$ g/cm^3, λ(Mo Kα) = 0.710 73 Å, μ(Mo Kα) = 2.18 cm^{-1}, final *R*1 and w*R*2 are 0.5072 and 0.8115 for 411 parameters and 9638 unique observed reflections with $I > 2\sigma(I)$.

(17) (a) Hayasi, Y.; Schwartz, J. *Inorg. Chem.* **1981**, *20*, 3473 and references therein. (b) Atagi, L. M.; Over, D. E.; McAlister, D. R.; Mayer, J. M. *J. Am. Chem. Soc.* **1991**, *113*, 870 and references therein. (c) Whinnery, L. L., Jr.; Henling, L. M.; Bercaw, J. E. *J. Am. Chem. Soc.* **1991**, *113*, 7575 and references therein. (d) Bäckvall, J. E.; Bökman, F.; Blomberg, M. R. A. *J. Am. Chem. Soc.* **1992**, *114*, 534.

(18) (a) Bottomley, F.; Sutin, L. *Adv. Organomet. Chem.* **1988**, *28*, 339. (b) Herrmann, W. A. *Angew. Chem., Int. Ed. Engl.* **1988**, *27*, 1297. (c) Nugent, W. A.; Mayer, J. M. *Metal−Ligand Multiple Bonds*; Wiley: New York, 1988. (d) Sheldon, R. A.; Kochi, J. M. *Metal-Catalyzed Oxidations of Organic Compounds*; Academic: New York, 1981. (e) Mimoun, H. In *Comprehensive Coordination Chemistry*; Wilkinson, G., Gillard, R. D., McCleverty, J. A., Eds.; Pergamon: Oxford, U.K., 1987; Vol. 6, Chapter 61.3, p 317.

(19) (a) Keramidas, A. D.; Miller, S. M.; Anderson, O. P.; Crans, D. C. *J. Am. Chem. Soc.* **1997**, *119*, 8091 and references therein. (b) Crans, D. C.; Jiang, F.; Chen, J.; Anderson, O. P.; Miller, M. M. *Inorg. Chem.* **1997**, *36*, 1038.

(20) (a) Ferguson, R.; Solari, E.; Floriani, C.; Osella, D.; Ravera, M.; Re, N.; Chiesi-Villa, A.; Rizzoli, C. *J. Am. Chem. Soc.* **1997**, *119*, 10104. (b) Laplaza, C. E.; Johnson, M. J. A.; Peters, J. C.; Odom, A. L.; Kim, E.; Cummins, C. C.; George, G. N.; Pickering, I. J. *J. Am. Chem. Soc.* **1996**, *118*, 8623 and the exhaustive list of references therein.

(21) (a) Hidai, M.; Mizobe, Y. *Chem. Rev.* **1995**, *95*, 1115. (b) Kisch, H.; Holzmeier, P. *Adv. Organomet. Chem.* **1992**, *34*, 67. (c) Sellmann, D. *Angew. Chem., Int. Ed. Engl.* **1974**, *13*, 639. (d) Gambarotta, S.; Floriani, C.; Chiesi-Villa, A.; Guastini, C. *J. Am. Chem. Soc.*, **1982**, *104*, 1918.

(22) (a) Sutton, D. *Chem. Rev.* **1993**, *93*, 995. (b) Kaplan, A. W.; Polse, J. L.; Ball, G. E.; Andersen, R. A.; Bergman, R. G. *J. Am. Chem. Soc.* **1998**, *120*, 11649.

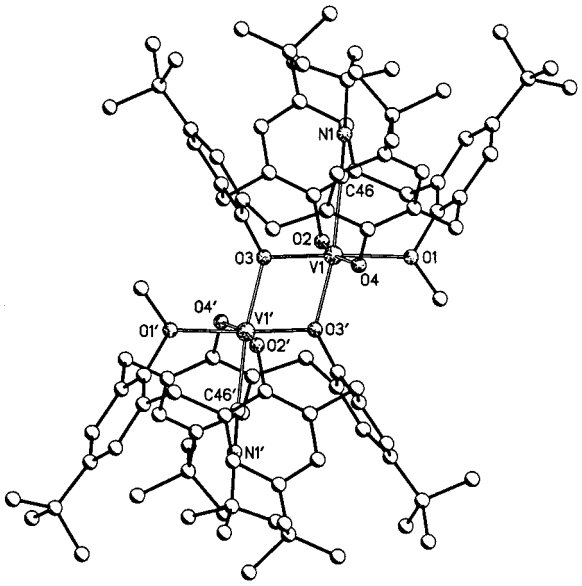

Figure 1. XP drawing of complex **3**. Hydrogens and solvent molecules are omitted for clarity.

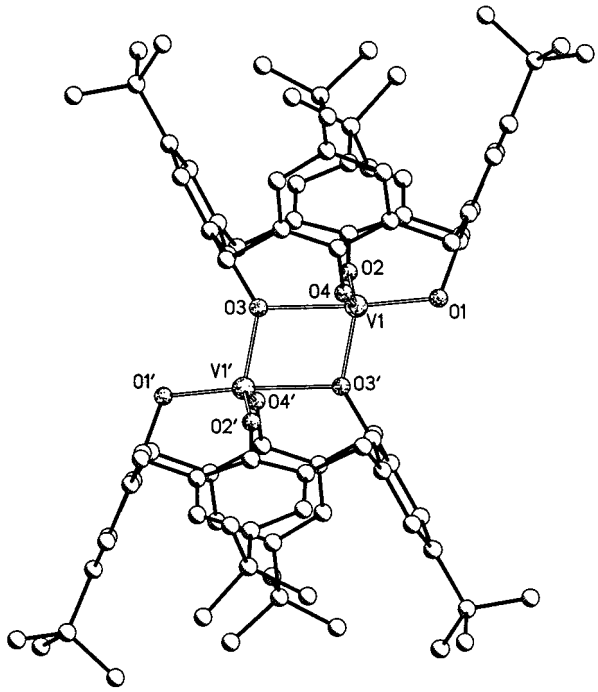

Figure 2. XP drawing of complex **7**. Hydrogens and solvent molecules are omitted for clarity.

0.410(3) Å, **10**]. The very short V−O(phenoxo) bond distances are in agreement with a quite efficient π-donation from the oxygen to the metal enhanced by the high oxidation state, +5, of the metal (Table 3). The poor σ bond donation from the methoxy group is shown by the rather long [V−O(1), 2.342(4), **9**; V−O(1), 2.397(5) Å, **10**] metal−oxygen interaction. The latter two structural parameters should be compared with the analogous ones in the V^{III} and V^{IV} dimethoxycalix[4]arene organometallic derivatives.[6] The V−methoxy distance is unusually long compared with those in the organometallic derivatives [$V-O_{av}$, 2.16 Å].[6] The V═O bond distance in **9** [1.586(4) Å] is similar to that in [$VOMes_3$] [1.575(4) Å].[8b] The bonding scheme for the diazomethane fragment shown for **10** in Scheme 2 is supported by the structural parameters (Table 3). The V(1)−N(1) bond distance [1.675(6) Å] closely approximates the value expected for a triple bond as in vanadium(V) species, which is further supported by the V(1)−N(1)−N(2) angle [160.3(5)°].[23] The two-electron reduction of diphenyldiazomethane gives rise to metallahydrazone with the bond distance sequence V(1)−N(1), 1.675(6), N(1)−N(2), 1.313(7), and C(46)−N(2), 1.310(8) Å, the N−N distance being slightly shorter than that expected for a single bond.[22a]

Chart 2

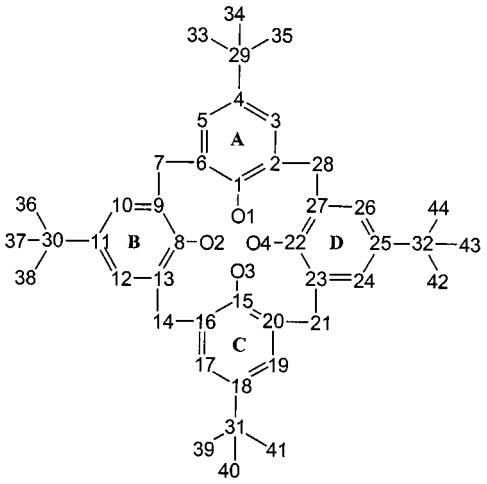

Table 2. Comparison of Relevant Conformational Parameters within the Calix-4-arene for **3**, **7**, **9**, and **10**

	3	**7**	**9**	**10**
(a) Angles between Planar Moieties[a]				
E ∧ **A**	57.4(3)	62.7(2)	63.2(2)	67.9(2)
E ∧ **B**	53.5(4)	32.9(3)	51.6(2)	54.0(2)
E ∧ **C**	56.4(3)	65.4(2)	62.3(1)	62.5(2)
E ∧ **D**	54.7(4)	53.7(2)	37.3(2)	28.0(3)
A ∧ **C**	66.3(5)	52.1(2)	54.5(2)	49.7(2)
B ∧ **D**	71.9(4)	86.6(2)	88.9(2)	81.9(2)
(b) Contact Distances between *para*-Carbon Atoms of Opposite Aromatic Rings				
C29···C31	10.32(2)	9.01(1)	9.407(8)	9.00(1)
C30···C32	10.50(2)	11.59(1)	11.30(1)	11.63(1)

[a] **E** (reference plane) refers to the least-squares plane defined by the bridging CH_2 [C7, C14, C21, C28]. **A**−**D** refer to the least-squares planes defined by the aromatic rings bonded to O1, O2, O3, and O4, respectively.

Table 3. Selected Bond (Å) and Angles (deg) for Complexes **3**, **7**, **9**, and **10**

	3	**7**	**9**	**10**
V1−O1	2.160(10)	1.835(5)	2.342(4)	2.397(5)
V1−O2	1.900(9)	1.742(5)	1.803(4)	1.816(5)
V1−O3	1.930(9)	2.198(5)	1.819(4)	1.844(5)
V1−O4	1.920(10)	1.790(5)	1.737(5)	1.781(5)
V1−O3[a]	2.084(9)	1.860(5)		
V1−O5			1.586(4)	
V1−N1				1.675(6)
V1−C46	2.157(14)			
N1−C46	1.148(15)			
N1−C47	1.47(2)			
N1−N2				1.313(7)
N2−C46				1.310(8)
N2−N1−V1				160.3(5)
C46−N2−N1				124.5(6)

[a] Symmetry operations used to obtain equivalent atoms: $-x, -y, -z$ (**3**); $-x+1, -y, -z$ (**7**).

(23) Nugent, W. A.; Mayer, J. M. *Metal-Ligand Multiple Bonds*; Wiley: New York, 1988; p 179.

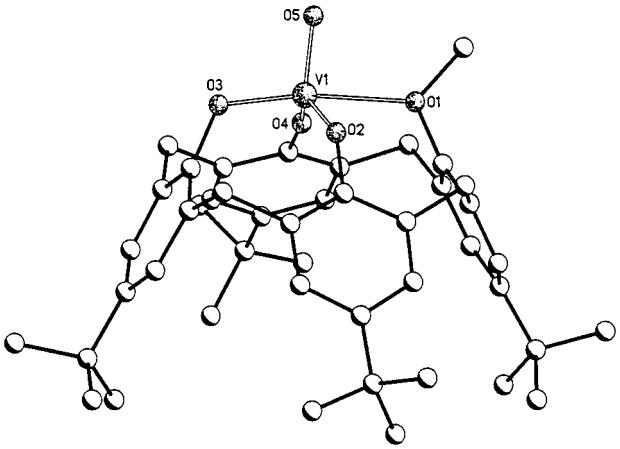

Figure 3. XP drawing of complex **9**. Hydrogens and solvent molecules are omitted for clarity.

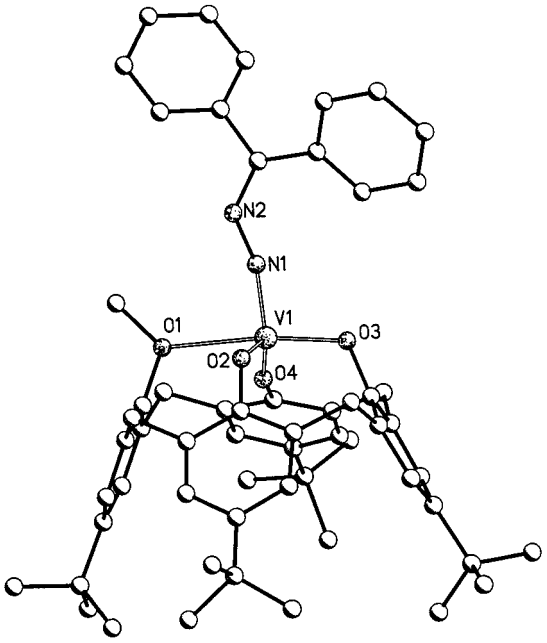

Figure 4. XP drawing of complex **10**. Hydrogens and solvent molecules are omitted for clarity.

Magnetic Studies. The magnetic susceptibilities of complexes **2**−**8** were measured in the temperature range 1.9−300 K, and those of **2**−**4** and **7** are shown in Figures 5 and 6.

(a) Vanadium(III) Complexes. The magnetic moment of **5** is essentially constant in the whole range of temperature showing only a small decrease below 10 K (due to zero-field-splitting), thus confirming the monomeric nature of this V^{III} compound. The temperature dependence of the magnetic moment of **2**−**4** shows a steady decrease from 300 to 1.9 K and is typical of antiferromagnetic coupled V^{III} dimers.[24] The data were fitted with the theoretical equation[25] based on the Heisenberg model $\mathbf{H} = -2J\mathbf{S}_1\cdot\mathbf{S}_2$ ($S_1 = S_2 = 1$),

$$\chi_{dim} = \frac{2Ng^2\mu_B{}^2}{kT}\,\frac{\exp(2x) + 5\exp(6x)}{1 + 3\exp(2x) + 5\exp(6x)}$$

where $x = J/kT$.

(24) Robles, J. C.; Matsukaza, Y.; Inomata, S.; Shimoi, M.; Mori, W.; Ogino, H. *Inorg. Chem.* **1993**, *32*, 13. Knopp, P.; Wieghardt, K. *Inorg. Chem.* **1991**, *30*, 4061.

(25) O'Connor, C. J. *Prog. Inorg. Chem.* **1982**, *29*, 203.

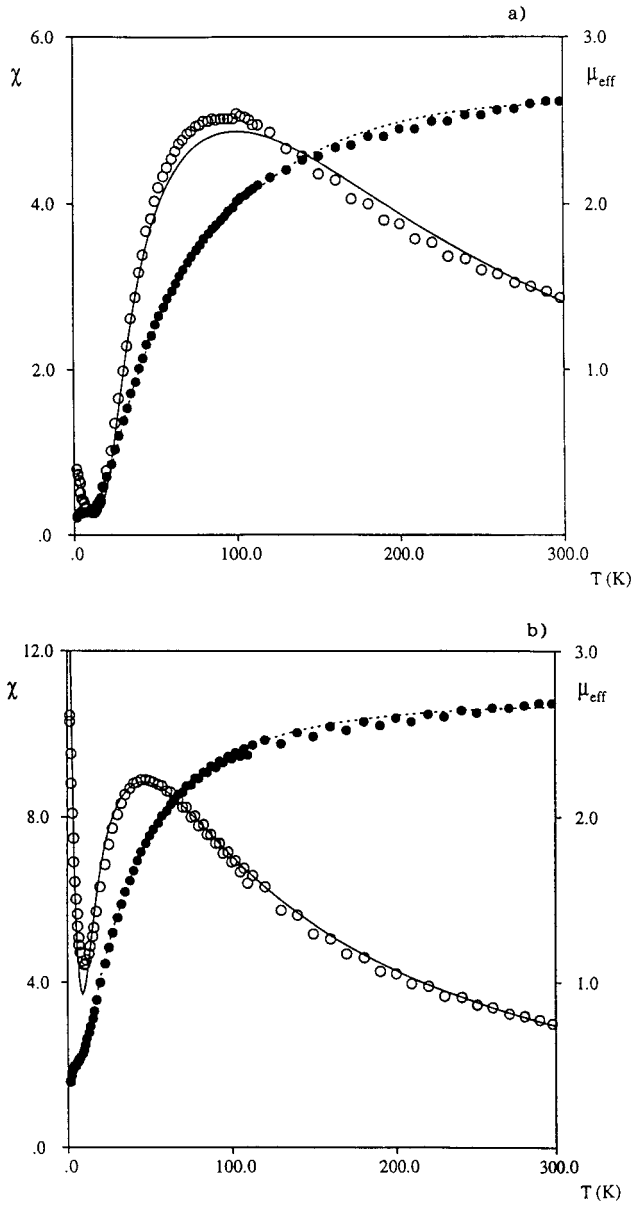

Figure 5. Magnetic susceptibility (○; 10^{-3} cm^3 mol^{-1}) and effective magnetic moment (●, μ_B) per vanadium vs temperature for (a) complex **2** and (b) complex **3**.

To obtain a good fit, we included a correction for a small quantity of monomeric V^{III} impurities, which were assumed to obey Curie law. The following equation is therefore used for the total susceptibility

$$\chi = \frac{1}{2}(1 - x)\chi_{dim} + x\,\frac{Ng'^2\mu_B{}^2S(S+1)}{3kT}$$

where $S = 1$, g' is the g-factor of the impurity (assumed 2.00), and x is the monomeric impurity fraction. The calculated best fit parameters are $g = 1.96$, $J = -76.4$ cm^{-1}, and $x = 2.2\%$ for **2**, $g = 1.99$, $J = -17.0$ cm^{-1}, and $x = 2.9\%$ for **3**, and $g = 1.98$, $J = -33.4$ cm^{-1}, and $x = 1.5\%$ for **4**.

Note that the antiferromagnetic coupling constant in these phenoxo-bridged V^{III}−V^{III} dimers strongly decreases upon trans coordination at the vanadium. This is probably due to the weakening of the bridging V−O bonds which decreases the orbital overlap of the d|p|d magnetic paths. The values observed for **3** and **4** are close to the values found for other alkoxo- or

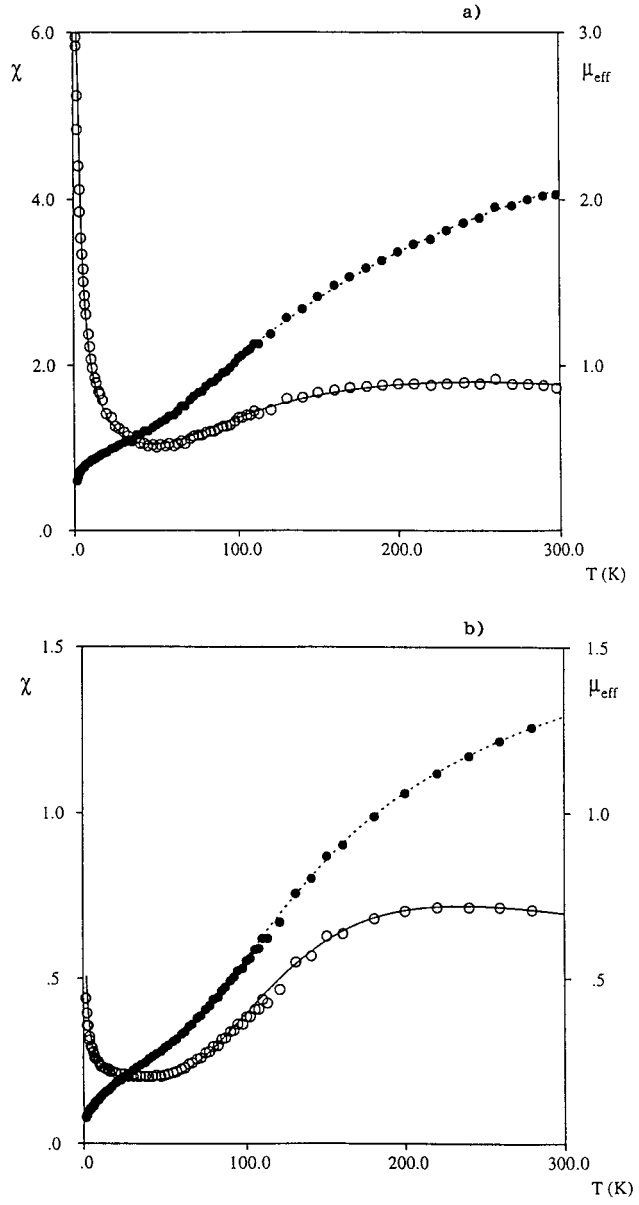

Figure 6. Magnetic susceptibility (○; 10^{-3} cm^3 mol^{-1}) and effective magnetic moment (●, μ_B) per vanadium vs temperature for (a) complex **4** and (b) complex **7**.

hydroxo-bridged V^{III} dimers, which fall in the range 10−40 cm^{-1}.[24] The magnetic moment of **6** remains essentially constant in the range 10−300 K showing only a small decrease below 10 K, thus indicating a negligible $V^{III}-V^{III}$ magnetic coupling through the dipyridyl bridge.

(b) Vanadium(IV) Complexes. The temperature dependence of the magnetic moment of **7** shows a continuous decrease from room temperature to 1.9 K and indicates an antiferromagnetic coupled V^{IV} dimer. The data were fitted with the Bleany−Bowers equation[25] based on the Heisenberg model $\mathbf{H} = -2J\mathbf{S}_1\cdot\mathbf{S}_2$ ($S_1 = S_2 = {}^1/_2$), accounting, again, for monomeric V^{IV} impurities:

$$\chi_{dim} = \frac{2Ng^2\mu_B{}^2}{kT}\frac{1}{3+\exp(-2J/kT)}$$

The calculated best fit parameters are $g = 1.71$, $J = -131.7$ cm^{-1}, and $x = 0.2\%$.

The magnetic moment of **8** is essentially constant in the range 10−300 K and shows only a small decrease below10 K indicating a negligible $V^{IV}-V^{IV}$ magnetic coupling through the hydroquinone bridge.

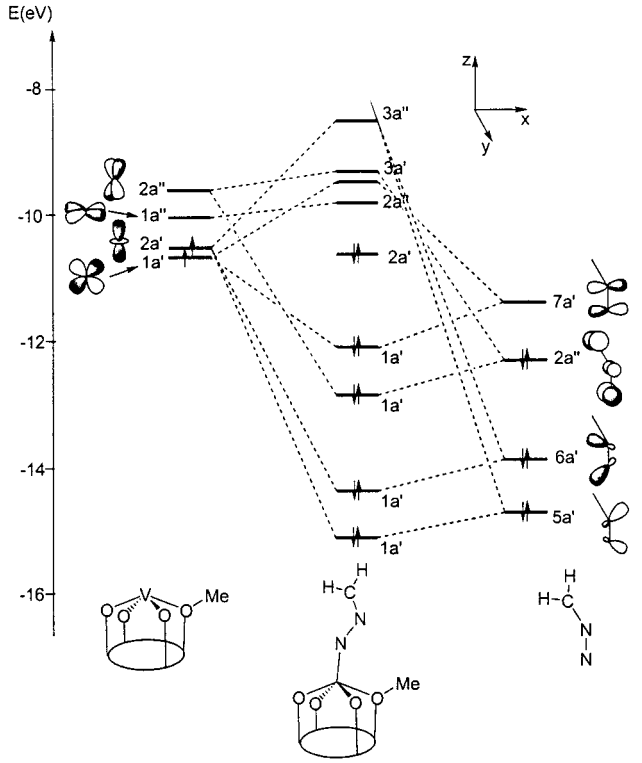

Figure 7. Orbital interaction diagram for the valence orbitals of **10**.

It is worth noting that the antiferromagnetic coupling constant, 131.7 cm^{-1}, observed for **7** is close to the values found for other phenoxo alkoxo or hydroxo bridged V^{IV} dimers which fall in the range 100−200 cm^{-1}.[26]

Extended Hückel Analysis. Extended Hückel calculations[27] were performed on a [calix[4](OMe)$(O)_3$V] fragment, simplifying the ligand to three phenoxo anions and one anisole molecule. This simplified model, with an imposed C_s symmetry, retains the main features of the whole ligand. In particular, the geometrical constraints on the O_4 set of donors atoms has been maintained by fixing the geometry of the phenoxo groups to the experimental structural parameters.

The frontier orbitals are reported on the left of Figure 7 and consist of four low-lying metal-based orbitals. We can distinguish two low-lying almost degenerate orbitals of a′ symmetry, i.e., the 1a′(d_{xz}), pointing into the plane containing the methylated oxygen, and the 2a′(d_{z^2}). Due to the stronger interaction with two phenoxo ligands in the *yz* plane, the 1a″(d_{yz}) is almost 1 eV higher in energy than the 1a ′(d_{xz}), with the 2a″(d_{xy}) orbital lying only 0.3 eV lower in energy.

The presence of low-lying empty metal d-orbitals in this hypothetical coordinatively unsatured species favors a strong coordination by a Lewis base, thus accounting for the easy coordination by coordinating solvent or for the dimerization. In particular, the two low-lying d_π orbitals allow a strong π interaction with suitable electron-rich ligands.

This has been exemplified by the coordination of diazomethane by the [calix[4]-(Ome)$(O)_3$V] fragment, a close model of complex **10**, since such coordination occurs with a simulta-

(26) Das, R.; Nanda, K. K.; Mukherjee, A. K.; Mukherjee, M.; Helliwell, M.; Nag, K. *J. Chem. Soc., Dalton Trans.* **1993**, 2241 and references therein.

(27) Hoffmann, R.; Lipscomb, W. N. *J. Chem. Phys.* **1962**, *36*, 2179. Hoffmann, R. *J. Chem. Phys.* **1963**, *39*, 1397.

neous two-electron reduction of the diazo functionality. The bonding between the metal fragment and the diazomethane moiety is illustrated by the interaction orbital diagram in Figure 7. On the extreme right of Figure 7 we show the frontier orbitals of the bent diazomethane ligand. The LUMO, 7a′, is mainly the antibonding p_x combination between the two nitrogens, and the HOMO, 2a″, is essentially a nonbonding orbital consisting of the out-of-phase combination of the p_y (N_1) and p_y (C) orbitals. Lower in energy are two orbitals of mainly nitrogen character, 5a′ and 6a′, made from a mixing of the in-phase p_x and p_z combinations, which share the lone pair of the terminal nitrogen. We see that the vanadium diazomethane bonding is achieved through three main orbital interactions: (i) a σ donation from the ligand 5a′ and 6a′ orbitals to 1a′(d_{z^2}); (ii) a π donation from the filled ligand 2a″ to the empty metal 2a″ (d_{yz}); (iii) a π retrodonation from the filled metal 1a′(d_{xz}) to the empty ligand 7a′. These interactions suggest a high bond order of the vanadium−nitrogen bond (between 2 and 3) in agreement with the observed short V−N distance of 1.675(6) Å (see Table 3).[23] Moreover, the high degree of back-donation to the 7a′ orbital of NN π^* character (1.48 electrons) leads to a significant weakening of the N−N bond as shown by the decrease of the overlap population from 1.11 in the free diazomethane to 0.74. This is in agreement with the observed long N−N distance of 1.31 Å (to be compared with 1.13 Å in free diazomethane).[28]

Acknowledgment. We thank the "Fonds National Suisse de la Recherche Scientifique" (Bern, Switzerland, Grant No. 20-53336.98), Ciba Specialty Chemicals (Basel, Switzerland), and Fondation Herbette (University of Lausanne, Lausanne, Switzerland (N.R.) for financial support.

Supporting Information Available: ORTEP drawings and tables of crystallographic data for **3**, **7**, **9**, and **10** (38 pages). This material is available free of charge via the Internet at http://pubs.acs.org.

IC990017M

(28) Brown, B. R. *The Organic Chemistry of Aliphatic Nitrogen Compounds*; Clarendon: Oxford, U.K., 1994; Chapter 13.